

TPE contribution being calculated in a different way and making use of Ref. 2 to resolve an ambiguity in sign.

<sup>8</sup>S. S. El-Ghabaty, S. N. Gupta, and J. Kaskas, *Phys. Rev. D* **1**, 249 (1970). The effect on the nucleon-nucleon phase parameters is determined by B. M. Barker and R. D. Haracz, *ibid.* **1**, 3187 (1970).

<sup>9</sup>R. E. Seamon, K. A. Friedman, G. Breit, R. D. Haracz, J. M. Holt, and A. Prakash, *Phys. Rev.* **165**, 1579 (1968). The isosinglet phase parameters are taken from Table IV and the isotriplet parameters from Table III. The uncertainties in these phase parameters,  $\Delta\delta_E$  in Eq. (7), are obtained by parallel shifts of the phase-energy curves within specified energy intervals.

<sup>10</sup>B. M. Barker, S. N. Gupta, and R. D. Haracz, *Phys. Rev.* **142**, 1144 (1966).

<sup>11</sup>The values  $g_\rho^2/4\pi\hbar^2 = 0.5^{+0.12}_{-0.1}$  and  $g_\omega^2/4\pi\hbar^2 = 3.5 \pm 1.2$  are given in P. J. Biggs, D. W. Braben, R. W. Clift, E. Gabathuler, P. Kitching, and R. E. Rand, *Phys. Rev.*

*Letters* **24**, 1197 (1970). Also see H. Alvensleben, U. Becker, W. K. Bertram, M. Chen, K. J. Cohen, R. T. Edwards, T. M. Knasel, R. Marshall, D. J. Quinn, M. Rohde, G. H. Sanders, H. Schubel, and S. C. C. Ting, *ibid.* **25**, 1273 (1970); S. C. C. Ting, in *Proceedings of the Fourteenth International Conference on High-Energy Physics, Vienna, 1968*, edited by J. Prentki and J. Steinberger (CERN, Geneva, Switzerland, 1968); J. Hamilton, *High-Energy Physics*, edited by E. H. S. Burhop (Academic, New York, 1967), Vol. I, Chap. 3, p. 193.

<sup>12</sup>The accurate determination of the pion-nucleon coupling strength by studying the long-ranged part of the nucleon-nucleon scattering interaction is discussed in G. Breit, M. Tischler, S. Mukherjee, and L. Lucas, *Proc. Natl. Acad. Sci. U.S.A.* **68**, 897 (1971); G. Breit, *ibid.* **63**, 223 (1969); *Nucl. Phys.* **B14**, 507 (1969).

PHYSICAL REVIEW D

VOLUME 4, NUMBER 5

1 SEPTEMBER 1971

## Test of Peripherality for $N$ - $N$ Scattering\*

Judith Binstock

*Physics Department and Cyclotron Institute, Texas A & M University, College Station, Texas 77843*

and

Ronald Bryan

*Physics Department, Texas A & M University, College Station, Texas 77843*

(Received 17 February 1971)

A semiquantitative test of peripherality in nucleon-nucleon scattering (up to 425 MeV lab kinetic energy) is carried out, using meson-nucleon coupling constants obtained from experiments other than nucleon-nucleon scattering. The model used is a pole model, plus a  $2\pi$ -exchange contribution, with geometric unitarization. The results show that a series of exchanges of increasingly larger masses gives an increasingly better description of the middle Taketani region ( $0.7 F < r \leq 2 F$ ). The series of exchanges considered is  $\pi$  exchange,  $\pi + 2\pi$  exchange, and  $\pi + 2\pi + \rho + \omega$  exchange. The exchange of  $\pi + 2\pi + \rho + \omega + \epsilon$  (715) is also considered, and an estimate is derived for the coupling constant  $g_{NN\epsilon}^2$ , assuming a width of  $\Gamma_\epsilon = 370$  MeV.

### I. INTRODUCTION

We propose to test the concept of peripherality in nucleon-nucleon elastic scattering in a semiquantitative fashion, using the present knowledge of meson-nucleon coupling constants obtained from experiments other than  $N$ - $N$  elastic scattering. To do this, we take for our model of the  $N$ - $N$  elastic scattering amplitude a sum of one-boson-exchange pole terms plus a  $2\pi$ -exchange term. With the meson-nucleon coupling constants determined from experiment, we have a "zero-parameter" model.

We follow in the spirit of the Taketani approach to  $N$ - $N$  scattering<sup>1</sup> where the nuclear force is divided up into three regions, an inner region (say

$0 < r \leq 0.7 F$ ), a middle region (say  $0.7 F < r \leq 2 F$ ), and an outer region ( $2 F < r < \infty$ ). We define distances through an impact-parameter relationship discussed in Sec. III, because experiments do not directly define distance in the usual sense, and because distances do not naturally come out of a pole model such as we use here. The one-pion-exchange (OPE) mechanism has been shown to dominate in the outer region.<sup>2-5</sup> In this paper we wish to see if the exchange of increasingly larger masses results in an increasingly better description of the middle Taketani region, the middle Taketani region being defined through the impact-parameter relationship of Sec. III. This is what we mean by a test of peripherality. The series of exchanges considered is  $\pi$  exchange,  $\pi + 2\pi$  ex-

change,  $\pi+2\pi+\rho+\omega$  exchange, and  $\pi+2\pi+\rho+\omega+\epsilon$  exchange. The numerical results are summarized in Sec. VI. The treatment of the wide  $\rho$  and  $\epsilon$  is described in Appendix B.

## II. QUALITATIVE TEST OF PERIPHERALITY

Consider as successive approximations to the  $N$ - $N$  elastic scattering amplitude a sum of terms representing the exchange of

- (1)  $\pi$ ,
- (2)  $\pi+2\pi$ ,
- (3)  $\pi+2\pi+\rho+\omega$ .

Note that these three approximations are numbered in order of increasingly larger mass of the exchanged system. The single-meson-exchange terms are pole terms, and their partial-wave projections are displayed in Appendix A. The  $2\pi$ -exchange contribution is taken from a previous paper<sup>6</sup> by one of the authors. This paper is hereafter referred to as paper I. The same geometric unitarization scheme is used here as in paper I, and is explained in Appendix A.

The values we use for the coupling constants, taken from experiment, are

$$\begin{aligned} g_{NN\pi}^2 &= 14.9, \\ g_{NN\rho}^2 &= 0.53, \quad f_\rho/g_\rho = 3.7, \\ g_{NN\omega}^2 &= 5, \quad f_\omega/g_\omega = -0.12. \end{aligned} \quad (2.1)$$

The value of  $g_{NN\pi}^2$  is taken from Ref. 7, an analysis of forward  $\pi^+p$  elastic scattering. The vector-meson Pauli to Dirac coupling constant ratios,  $f_\rho/g_\rho$  and  $f_\omega/g_\omega$ , are derived under the assumption that the  $\rho$  and  $\omega$  saturate the isovector and isoscalar electromagnetic nucleon form factors, respectively, at zero momentum transfer. The same assumption applied to the  $e^+e^-$  colliding beam results reported by Ting<sup>8</sup> yields  $g_{NN\rho}^2 = 0.53 \pm 0.04$  and  $g_{NN\omega}^2 = 4.69^{+1.24}_{-0.81}$ . The exchange of an  $\eta(549)$  is omitted because with a coupling constant of  $g_{NN\eta}^2 < 0.002$ ,<sup>9</sup> its contribution is negligible. The masses used (from Ref. 10) are

$$\begin{aligned} m_\pi &= \text{averaged pion mass} = 137 \text{ MeV}/c^2, \\ M &= \text{averaged nucleon mass} = 939 \text{ MeV}/c^2, \\ m_\rho &= 765 \text{ MeV}/c^2, \quad \text{width } \Gamma_\rho = 117 \text{ MeV}, \\ m_\omega &= 783 \text{ MeV}/c^2. \end{aligned} \quad (2.2)$$

The treatment of the wide  $\rho$  is given in Appendix B.

The  $2\pi$ -exchange contribution is described in detail in paper I. It is derived by approximating the  $N\bar{N} \rightarrow \pi\pi$  amplitude by a sum of  $N(938)$  and  $\Delta(1236)$  pole terms, and then using  $u$ -channel ( $N\bar{N} \rightarrow N\bar{N}$  channel) unitarity and crossing to determine the

contribution to the  $u$  discontinuity of the  $NN \rightarrow NN$  amplitude due to  $2\pi$  exchange. Then a dispersion relation for the  $NN \rightarrow NN$  amplitude is written, employing a cutoff  $u_c$  in the momentum-transfer variable  $u$ . For the  $2\pi$ -exchange contribution in this paper we use values of  $m_\pi$  and  $M$  as in (2.2) above, plus

$$\begin{aligned} M_\Delta &= 1236 \text{ MeV}/c^2, \quad \text{width } \Gamma_\Delta = 120 \text{ MeV}, \\ u_c &= (3.5m_\pi)^2. \end{aligned} \quad (2.3)$$

The three successive approximations described in the first paragraph of this section yield the nuclear-bar phase parameter curves labeled 1, 2, and 3 in Fig. 1. (Curve 4 represents the exchange of  $\pi+2\pi+\rho+\omega$  and an  $\epsilon$  of mass 715 MeV/ $c^2$  and width 370 MeV, with the coupling constant  $g_{NN\epsilon}^2$  searched for the best fit. This curve will be discussed in Sec. V.)

In Fig. 1, note the general trend toward improved fit for curve 1, one-pion exchange, as we go to lower energies in a single partial wave, and also as we go to higher partial waves. The same holds for curves 2 and 3. Since classically

$$L = pr, \quad (2.4)$$

where  $L$  is the orbital angular momentum,  $p$  is the c.m. momentum of either nucleon, and  $r$  is the impact parameter, we can say roughly that higher partial waves or lower energies correspond to bigger impact parameters. So each one of the successive approximations 1, 2, 3 shows improvement as the impact parameter considered is increased.

There is also an over-all trend of improvement in fit when we add exchanges of higher-mass systems, i.e., as we progress from approximation 1 to approximation 2 and from 2 to 3, although this is more easily seen after we introduce a quantity representing goodness of fit.

## III. QUANTITATIVE TEST OF PERIPHERALITY

We determine  $\chi^2$  from a MacGregor-Arndt-Wright second-derivative error matrix.<sup>11</sup> For small deviations from the experimentally determined phase shifts, this  $\chi^2$  is the same as would result from using the actual  $N$ - $N$  data. While this is not true when  $\chi^2$  is large, we are going to assume that the actual goodness-of-fit is monotonically related to the value of  $\chi^2$  obtained from the second-derivative error matrix.

Assigning the masses and coupling constants as in Eqs. (2.1)–(2.3), we plot in Fig. 2  $\chi^2/(\text{datum})$  as a function of  $l_{\min}$ , for the same cases 1–4 as in Fig. 1, where  $l_{\min}$  is the lowest partial wave fit. For example, when  $l_{\min} = 2$ , we fit  $D$ ,  $F$ ,  $G$ , and  $H$  waves, as well as the coupling parameters  $\epsilon_2$

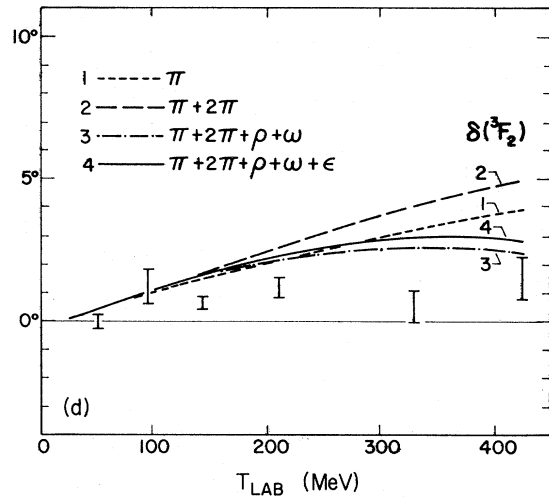
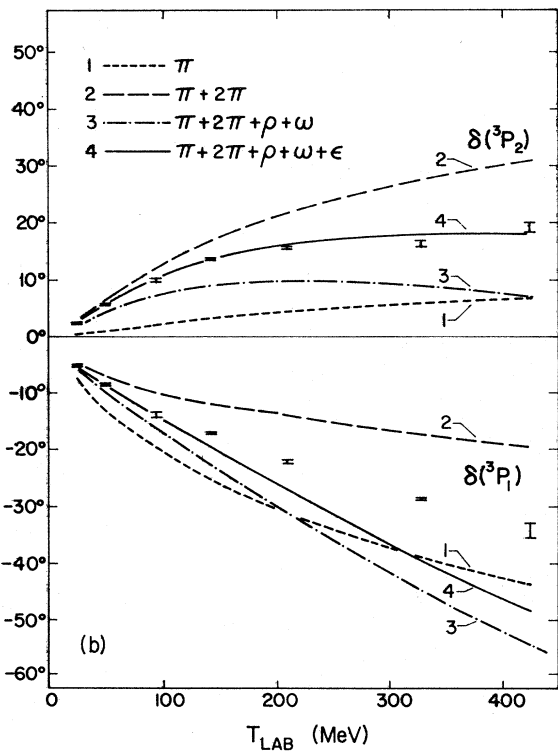
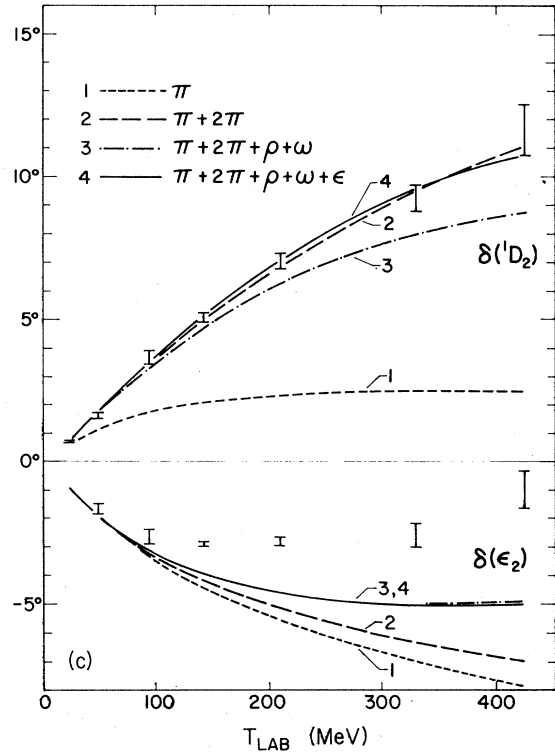
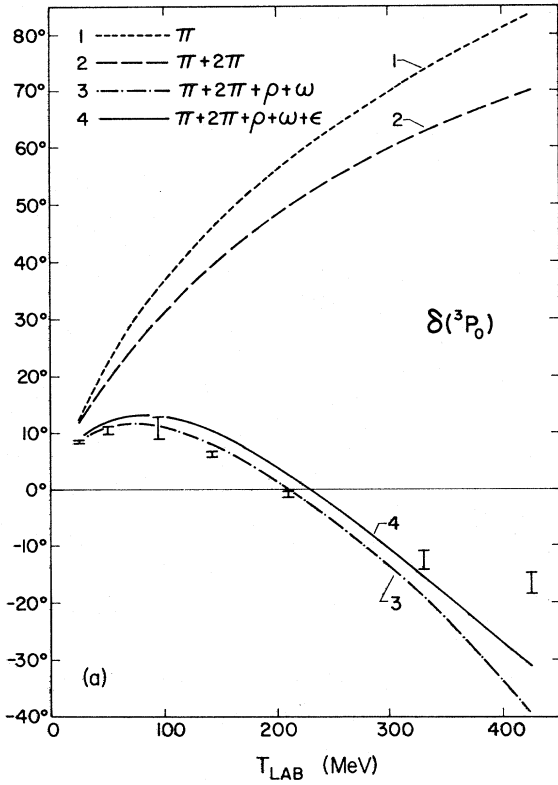


Fig. 1 (Continued). Caption on p. 1345.

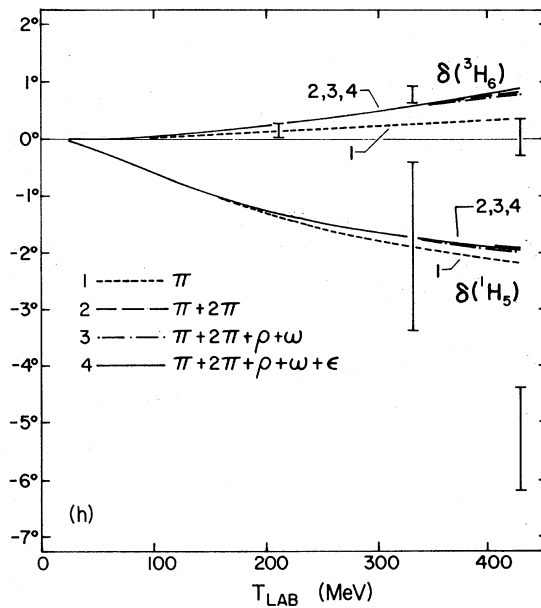
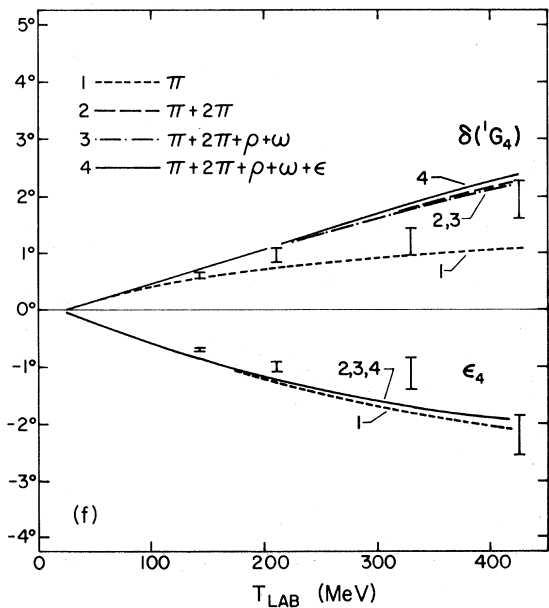
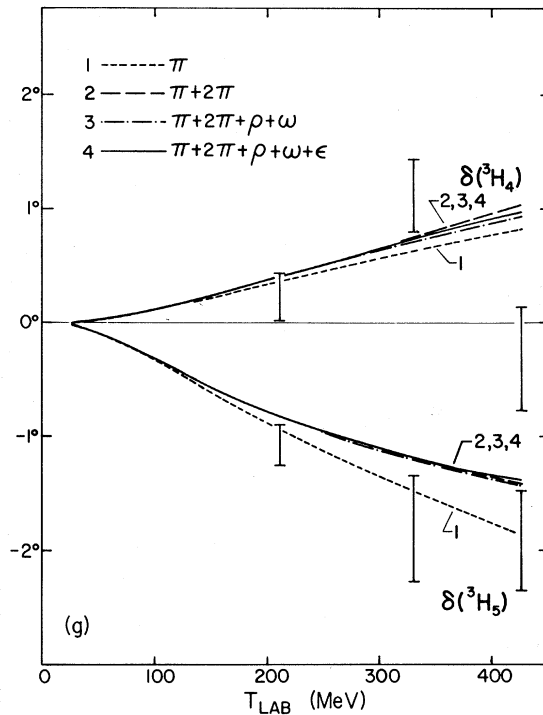
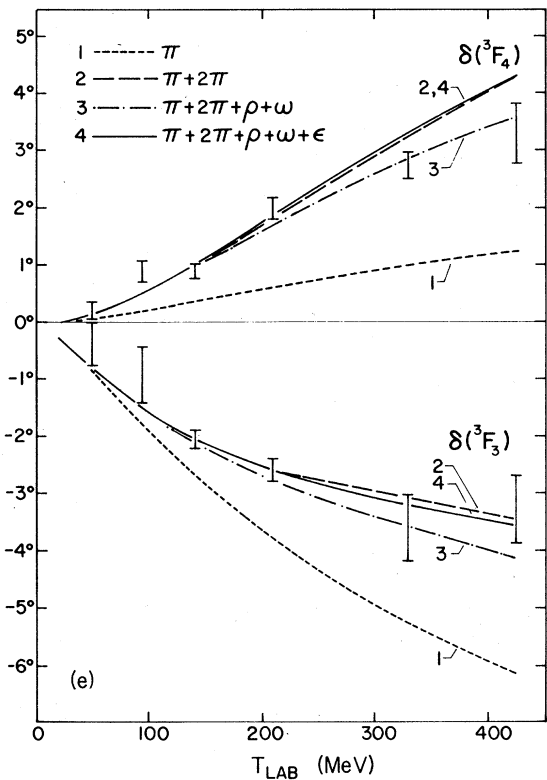


Fig. 1 (Continued). Caption on next page.

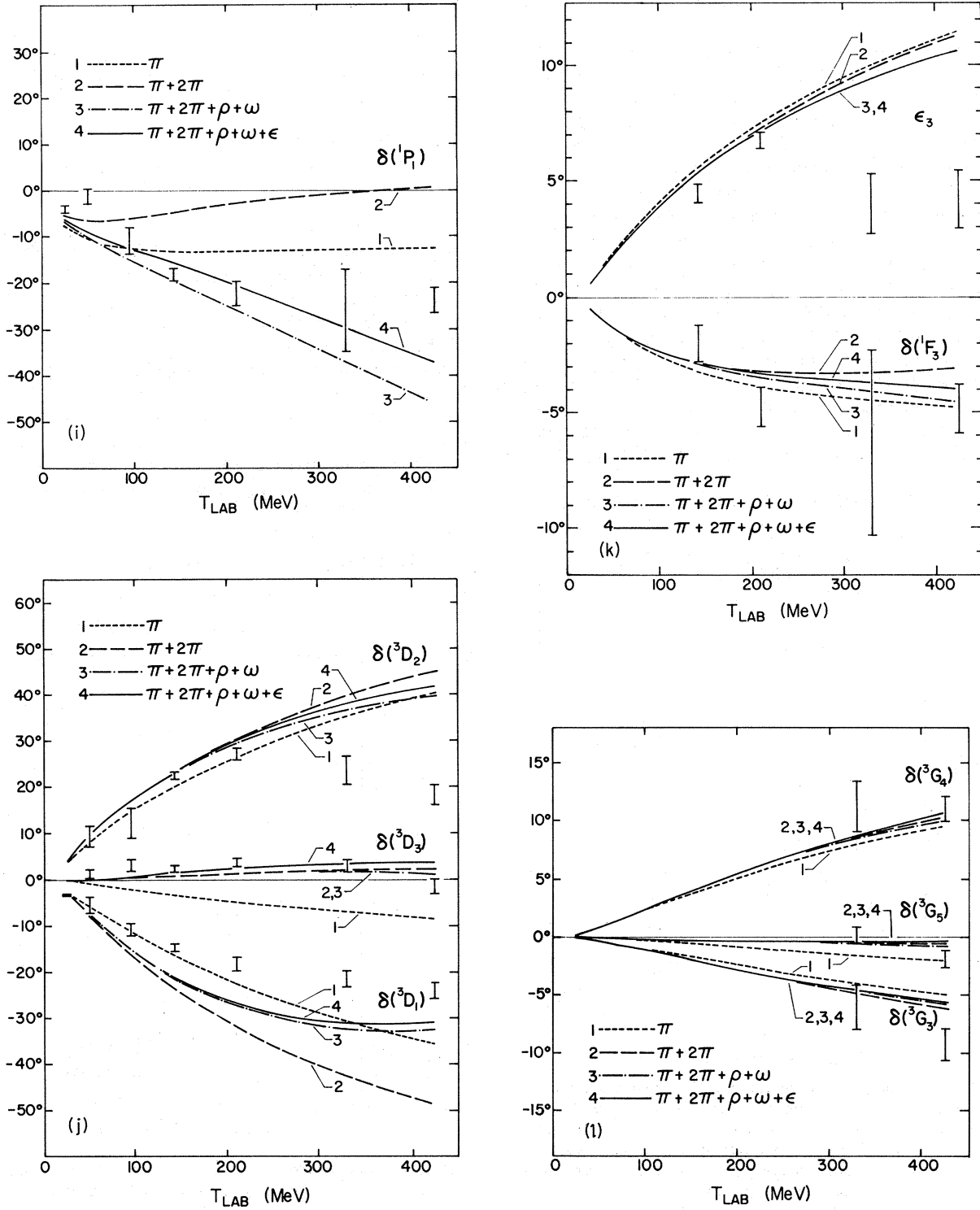


FIG. 1. Nuclear-bar phase parameters (in deg) for  $N$ - $N$  scattering, for four different models:  $\pi$  exchange,  $\pi+2\pi$  exchange,  $\pi+2\pi+\rho+\omega$  exchange, and  $\pi+2\pi+\rho+\omega+\epsilon$  exchange. The  $2\pi$ -exchange contribution is taken from paper I. The parameters used are given in Eqs. (2.1)–(2.3) of this paper,  $m_\epsilon = 715 \text{ MeV}/c^2$  and  $\Gamma_\epsilon = 370 \text{ MeV}$ . For curve 4,  $\xi_{NN\epsilon}^2$  is searched for a best fit to the  $P$  through  $H$  waves ( $\epsilon_1$  excluded from the fit). The data points are shown and are taken from Ref. 13.

through  $\epsilon_5$ . (Each  $\epsilon_j$  is treated as an  $l=J$  partial-wave parameter.) The higher partial waves ( $l \geq 6$ ) were treated in the partial-wave analysis<sup>12</sup> of the data as coming solely from OPE. The lower partial-wave parameters, those lower than the value of  $l_{\min}$  on the graph, are allowed to search to whatever value minimizes  $\chi^2$ . In no case do we attempt to fit S waves or the coupling parameter  $\epsilon_1$ , since the geometric unitarization scheme is inadequate to describe these, and also since these parameters are so sensitive to the short-range forces not given by the model. When  $l_{\min} = 1$ ,  $\epsilon_1$  is excluded from the fit, and is freed to search. We fit data from 1292  $pp + np$  data points and seven energies: 25, 50, 95, 142, 210, 330, and 425 MeV.

Since the experimental error on  $g_{NN\omega}^2$  is so large (in Sec. II we derived  $g_{NN\omega}^2 = 4.69_{-0.81}^{+1.24}$  from Ref. 8), we plot in Fig. 2 the results for  $g_{NN\omega}^2 = 4, 5, 6$ . Only for  $l_{\min} = 1$  is there any noticeable variation in  $\chi^2/(\text{datum})$ , and here the lowest value of  $g_{NN\omega}^2$  is favored.

Extending the classical impact-parameter rela-

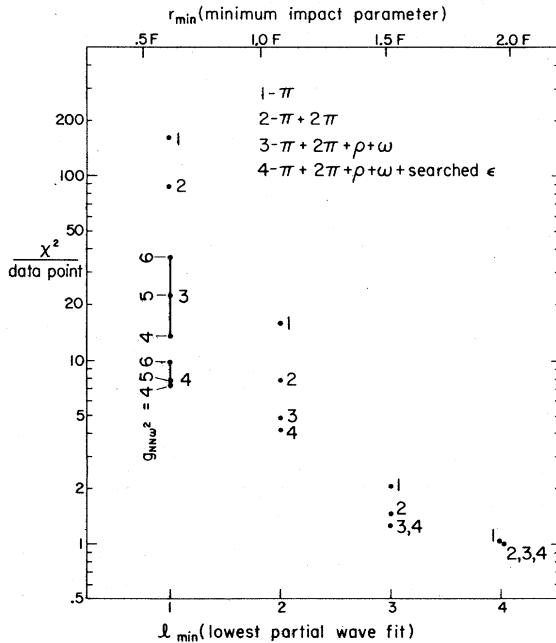


FIG. 2. Goodness-of-fit for four different models of  $N-N$  scattering:  $\pi$  exchange,  $\pi+2\pi$  exchange,  $\pi+2\pi+\rho+\omega$  exchange, and  $\pi+2\pi+\rho+\omega+\epsilon$  exchange; calculated for a fit to the  $5 \geq l \geq l_{\min}$  partial waves, using the second-derivative matrix of Ref. 12 (based on 1292  $pp + np$  data points at 25, 50, 95, 142, 210, 330, and 425 MeV). The  $2\pi$ -exchange contribution is taken from paper I. The parameters used are as in Eqs. (2.1)–(2.3) of this paper, with  $m_\epsilon = 715 \text{ MeV}/c^2$  and  $\Gamma_\epsilon = 370 \text{ MeV}$ . Values are shown for  $g_{NN\omega}^2 = 4, 5, \text{ and } 6$ , although only for  $l_{\min} = 1$  is there any perceptible difference. The coupling constant  $g_{NN\epsilon}^2$  is searched to minimize  $\chi^2$  for each value of  $l_{\min}$  and for each value of  $g_{NN\omega}^2$ .

tion Eq. (2.4) to

$$[l(l+1)]^{1/2} \hbar = p r, \quad (3.1)$$

where  $l$  is the orbital angular momentum quantum number, we get

$r_{\min}$  = minimum impact parameter

$$\begin{aligned} &= [l_{\min}(l_{\min}+1)]^{1/2} \hbar / p \\ &= 0.44 [l_{\min}(l_{\min}+1)]^{1/2} F, \end{aligned} \quad (3.2)$$

which is shown on the top scale of Fig. 2.<sup>13</sup> (We have used the fact that the highest-energy fit is 425 MeV.) So scanning from left to right in Fig. 2 corresponds to looking at increasingly large impact parameters.

Note the obvious improvement now, as we progress from approximation 1 to approximation 2, and from 2 to 3, as well as the improvement for each one of the 3 approximations as the minimum impact parameter is increased. The points labeled 4 represent the exchange of  $\pi+2\pi+\rho+\omega$  + an  $\epsilon$  (mass = 715 MeV/ $c^2$ , width = 370 MeV) with the coupling constant  $g_{NN\epsilon}^2$  searched for a best fit. The significance of these points will be discussed

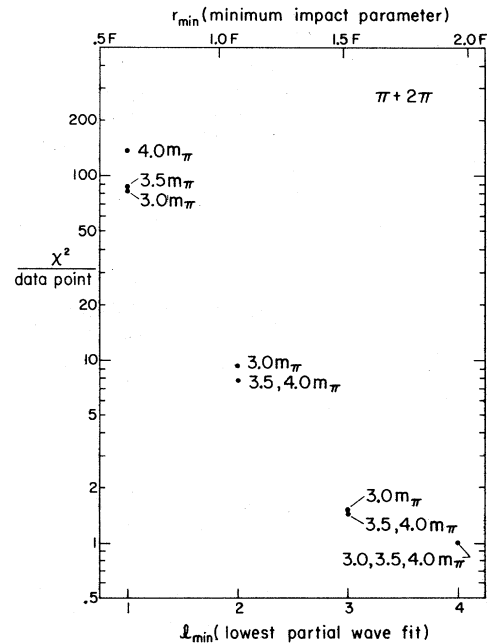


FIG. 3. Goodness-of-fit for the approximation of the  $N-N$  amplitude by a  $\pi+2\pi$  exchange model, with  $2\pi$  cut-offs  $u_c^{1/2}$  (defined in paper I) of  $3.0m_\pi$ ,  $3.5m_\pi$ , and  $4.0m_\pi$ , as indicated. The other parameters are as found in Eqs. (2.1)–(2.3) of this paper.  $\chi^2$  is determined from a fit to the  $5 \geq l \geq l_{\min}$  partial waves, using the second-derivative matrix of Ref. 12. A comparison of Fig. 3 with Fig. 2 indicates the degree of sensitivity of the model to variations in the  $2\pi$  cutoff parameter.

in Sec. V.

The values of  $\chi^2/(\text{datum})$  shown for  $l_{\min} = 1$  correspond to the curves 1 to 4 shown in Fig. 1.

#### IV. SENSITIVITY TO $2\pi$ -EXCHANGE MODEL USED

The discussion in paper I of the  $2\pi$ -exchange contribution concludes that a cutoff in the momentum transfer of between  $(3m_\pi)^2$  and  $(4m_\pi)^2$  is a reasonable one to choose. In Fig. 3, we show the  $\chi^2/(\text{datum})$  resulting from approximation 2,  $\pi + 2\pi$  exchanged, for three different choices of cutoff:  $u_c = (3.0m_\pi)^2$ ,  $(3.5m_\pi)^2$ , and  $(4.0m_\pi)^2$ . A comparison of this plot with that of Fig. 2 will show that the conclusions drawn from Fig. 2 still hold. There is no great sensitivity to the value of the momentum-transfer cutoff in this range, as far as a test of peripherality is concerned.

#### V. $\epsilon$ -EXCHANGE CONTRIBUTION

We cannot reasonably leave out the  $\epsilon(715)$ -exchange contribution, while including the higher mass  $\rho(765)$  and  $\omega(783)$ . But without a good experimental determination of the strength of the coupling of the  $\epsilon$ , or even of its mass or width, we can only say what values are consistent with the notion of peripherality. If we take the values  $m_\epsilon = 715 \text{ MeV}/c^2$  (from Ref. 10) and  $\Gamma_\epsilon = 370 \text{ MeV}$  (see Ref. 14), then we can say what values of  $g_{NN\epsilon}^2$  will optimize the fit to the data. (See Fig. 4 for a plot of the results.) The treatment of the wide  $\epsilon$  is given in Appendix B.

We represent the  $N$ - $N$  scattering amplitude as the exchange of  $\pi + 2\pi + \rho + \omega + \epsilon$ , with the  $\epsilon$  parameters as above and the other parameters as in Eqs. (2.1)–(2.3) (with  $g_{NN\omega}^2 = 5$ ); then we search on  $g_{NN\epsilon}^2$ . The value that gives the best fit for  $l_{\min} = 1$  ( $P$  waves and higher fit) is  $g_{NN\epsilon}^2 = 3.2$ . The resulting phase shifts are plotted as curve 4 in Fig. 1. The resulting  $\chi^2/(\text{datum})$  is the point in Fig. 2 labeled 4 and at  $l_{\min} = 1$ , i.e.,  $\chi^2/(\text{datum}) = 7.8$ . This is the lowest value we can get (for this model) for  $\chi^2/(\text{datum})$ , fitting  $P$  waves and higher, leaving the  $\epsilon$  coupling constant  $g_{NN\epsilon}^2$  free to search, and fixing the other parameters as described. Releasing those parameters and letting them search would of course give a lower  $\chi^2/(\text{datum})$ , but this would represent a less stringent test of peripherality.

The values of  $g_{NN\epsilon}^2$ , namely  $(g_{NN\epsilon}^2)_{\min}$ , which minimize  $\chi^2/(\text{datum})$  for a fit to the  $5 \geq l \geq l_{\min}$  partial waves, are shown in Fig. 4. The error bars represent the change in  $g_{NN\epsilon}^2$  which would increase  $\chi^2$  by 1. We note that  $(g_{NN\epsilon}^2)_{\min}$  depends systematically on the value of  $g_{NN\omega}^2$ , which is not well determined experimentally. A plot of  $(g_{NN\epsilon}^2)_{\min}$  vs

$g_{NN\omega}^2$  for a  $\pi + 2\pi + \rho + \omega + \epsilon$ -exchange model (the other coupling constants held fixed), with  $D$  waves and higher fitted to the data, in fact yields Fig. 5. The change in  $g_{NN\epsilon}^2$  which changes  $\chi^2$  by 1 is indicated by the error bars.

We do not regard any of the considerations of this section as other than a crude determination of  $g_{NN\epsilon}^2$ , because of the crudities of the model, and because of the many contributions to the  $N$ - $N$  scattering amplitude other than  $\epsilon$  exchange, some of which (like  $3\pi$  exchange) are not even considered. Nevertheless, should one want an estimate of  $g_{NN\epsilon}^2$ , the value for  $l_{\min} = 2$  (Table I) is the most likely candidate: For  $l_{\min} = 1$ , our geometric unitarization scheme begins to break down, and peripherality (representation of the nuclear force by the sum of a few exchanges) also begins to break down; while for  $l_{\min} = 3$  or 4, the phase parameters are insensitive to intermediate-range processes, and yield little information on  $g_{NN\epsilon}^2$  (see Sec. VI). For  $g_{NN\omega}^2 = 5 \pm 1$  (see Sec. II), we then estimate (from Table I) that

$$g_{NN\epsilon}^2 = 6 \pm 1. \quad (5.1)$$

It appears then that inclusion of the  $2\pi$ -exchange contribution does not eliminate the need for an

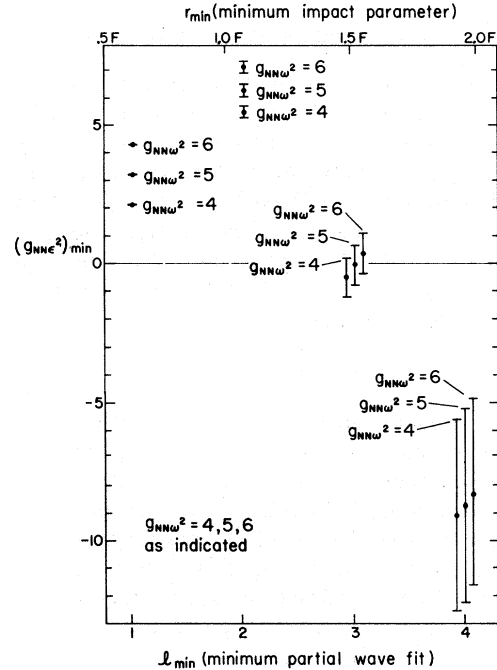


FIG. 4. Values of  $g_{NN\epsilon}^2$  which minimize  $\chi^2$  for a fit to the  $5 \geq l \geq l_{\min}$  partial waves, for a given  $l_{\min}$  and a given  $g_{NN\omega}^2$ . The model is that of  $\pi + 2\pi + \rho + \omega + \epsilon$  exchange, with parameters taken from Eqs. (2.1)–(2.3). The error bars represent the increment in  $(g_{NN\epsilon}^2)_{\min}$  which increases  $\chi^2$  by 1.

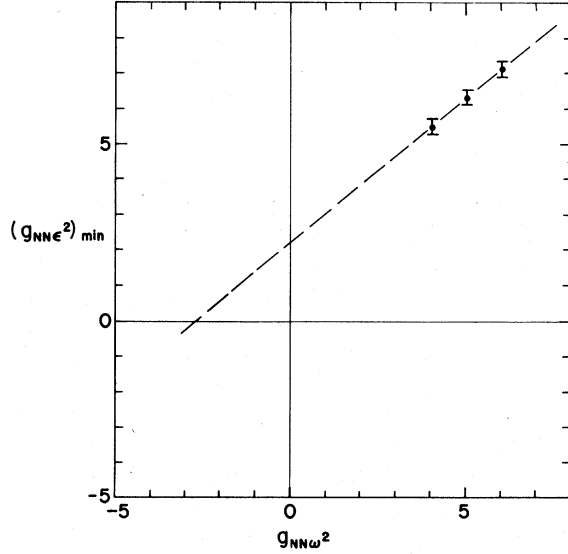


FIG. 5. The value of  $g_{NN\epsilon^2}$  which minimizes  $\chi^2$ , as a function of  $g_{NN\omega^2}$ , for a fit to the  $5 \geq l \geq 2$  partial waves. The error bars represent the increment in  $g_{NN\epsilon^2}$  which increases  $\chi^2$  by 1. The model used is that of  $\pi + 2\pi + \rho + \omega + \epsilon$  exchange.

isoscalar scalar meson-exchange contribution in fitting the  $N$ - $N$  data.

## VI. NUMERICAL SUMMARY

A summary of the numerical results of this paper, for the various approximations to the  $N$ - $N$  scattering amplitude, is given in Table II. Note that  $(g_{NN\epsilon^2})_{\min}$  is the value which minimizes  $\chi^2$ , the other parameters fixed as given. The error in  $(g_{NN\epsilon^2})_{\min}$  is the increment in  $g_{NN\epsilon^2}$  which increases  $\chi^2$  by 1. For our model,  $\chi^2$  is linear in  $[g_{NN\epsilon^2} - (g_{NN\epsilon^2})_{\min}]^2$ , so that Table II can be used to calculate  $\chi^2$  for any value of  $g_{NN\epsilon^2}$ .

## VII. CONCLUSION

For a model of nucleon-nucleon elastic scattering consisting of a sum of a one-meson-exchange pole terms plus a  $2\pi$ -exchange term, using meson-nucleon coupling constants from experiments other than nucleon-nucleon elastic scattering, the fit to the data shows a consistent improvement as one proceeds from smaller to larger impact parameters and from smaller to larger exchanged mass

TABLE I. Optimal values of  $g_{NN\epsilon^2}$ , for  $l_{\min} = 2$ .

$g_{NN\omega^2}$	$g_{NN\epsilon^2}$
4	$5.5 \pm 0.22$
5	$6.3 \pm 0.22$
6	$7.1 \pm 0.22$

systems. The data examined are from Ref. 12 and include 1292  $pp + np$  data points from the seven energies 25, 50, 95, 142, 210, 330, and 425 MeV.

It was already known that for very large impact parameters the OPE mechanism is a good representation of  $N$ - $N$  elastic scattering; now the evidence suggests that for an intermediate range of impact parameter, the representation of the  $N$ - $N$  elastic scattering amplitude by the sum of a few one-meson-exchange terms ( $\pi + \rho + \omega + \epsilon$ ) plus a  $2\pi$ -exchange term is a reasonable model. There appears to be a "convergence" of the series of exchanges, as can be seen in Fig. 2. A better dynamical model than a pole model is needed, of course, for the smaller impact parameters.

## ACKNOWLEDGMENT

We are grateful to Dr. Richard A. Arndt for making available a deck of his second-derivative matrix for  $N$ - $N$  scattering, and to Dr. Alex Gersten for his help in treating wide-meson exchange.

## APPENDIX A: PARTIAL-WAVE PROJECTIONS OF THE ONE-BOSON-EXCHANGE CONTRIBUTIONS TO $N$ - $N$ SCATTERING

We list the one-boson-exchange partial-wave projections. In the following  $p$  is the c.m. momentum of either nucleon, and is given by

$$p^2 = \frac{1}{2} M T_{\text{lab}}, \quad (\text{A1})$$

where  $M$  is the nucleon mass and  $T_{\text{lab}}$  is the lab kinetic energy of the incident nucleon,

$$x_0 = 1 + m^2/2p^2, \quad (\text{A2})$$

where  $m$  is the meson mass, and

$$a = [p/(E+M)]^2, \quad (\text{A3})$$

where  $E = (p^2 + M^2)^{1/2}$ . The amplitudes  $f_0^J$ ,  $f_1^J$ ,  $f_{L=J-1}^J$ ,  $f_{L=J+1}^J$ , and  $f_{J-1, J+1}^J$  represent partial-wave projections of  $(\underline{S}-1)/2i$ :

$$f_0^J = \langle J, L=J, S=0 | (\underline{S}-1)/2i | J, L=J, S=0 \rangle, \quad (\text{A4a})$$

$$f_1^J = \langle J, L=J, S=1 | (\underline{S}-1)/2i | J, L=J, S=1 \rangle, \quad (\text{A4b})$$

$$f_{L=J-1}^J = \langle J, L=J-1, S=1 | (\underline{S}-1)/2i | J, L=J-1, S=1 \rangle, \quad (\text{A4c})$$



TABLE II. Goodness of fit for various approximations to the  $N-N$  scattering amplitude.

Exchanges <sup>a</sup>	$g_{NN\pi}^2$	$u_c^{1/2}$	$g_{NN\rho}^2$	$g_{NN\omega}^2$	$(g_{NN\epsilon}^2)_{\min}$	$l_{\min}=1$	$\chi^2/\text{datum}^b$				
							2	3	4 <sup>c</sup>		
$\pi$	14.9					160.0	15.7	2.04	1.01		
$\pi+2\pi$	14.9	$3.0m_\pi$				82.5	9.21	1.50	0.98		
		$3.5m_\pi$				86.8	7.73	1.42	0.98		
		$4.0m_\pi$				137.0	7.74	1.44	0.99		
$\pi+2\pi+\rho+\omega$	14.9	$3.5m_\pi$	0.53	4.0		13.5	4.66	1.25	0.97		
				5.0		22.1	4.78	1.24	0.97		
				6.0		35.5	4.92	1.23	0.97		
$\pi+2\pi+\rho+\omega$ +searched $\epsilon$	14.9	$3.5m_\pi$	0.53	4.0	$2.11 \pm 0.024$	7.31					
					$5.51 \pm 0.22$		4.16				
					$-0.46 \pm 0.72$			1.25			
					$-9.05 \pm 3.5$				0.97		
						5.0	$3.21 \pm 0.024$	7.77			
							$6.33 \pm 0.22$		4.12		
							$-0.03 \pm 0.72$			1.24	
							$-8.68 \pm 3.5$				0.97
						6.0	$4.31 \pm 0.024$	9.72			
							$7.15 \pm 0.22$		4.08		
			$0.40 \pm 0.72$			1.23					
			$-8.30 \pm 3.5$				0.97				

<sup>a</sup>We have used  $f_\rho/g_\rho=3.7$  and  $f_\omega/g_\omega=-0.12$  throughout, where applicable, as well as  $m_\pi=137$  MeV/ $c^2$ ,  $M=939$  MeV/ $c^2$ ,  $m_\rho=765$  MeV/ $c^2$ ,  $m_\omega=783$  MeV/ $c^2$ ,  $m_\epsilon=715$  MeV/ $c^2$ ,  $\Gamma_\rho=117$  MeV, and  $\Gamma_\epsilon=370$  MeV.

<sup>b</sup> $\chi^2$  is calculated from the MacGregor-Arnt-Wright second-derivative error matrix.<sup>11</sup> It represents an energy-independent fit to 1292  $pp+np$  data points from seven energies: 25, 50, 95, 142, 210, 330, and 425 MeV.

<sup>c</sup>The phase parameters which we fit are those for which  $5 \geq l \geq l_{\min}$ .

$$f_{L=J+1} = \langle J, L=J+1, S=1 | (\underline{S}-\underline{1})/2i | J, L=J+1, S=1 \rangle, \quad (\text{A4d})$$

$$f_{J-1, J+1} = \langle J, L=J-1, S=1 | (\underline{S}-\underline{1})/2i | J, L=J+1, S=1 \rangle, \quad (\text{A4e})$$

where  $\underline{S}$  is the scattering matrix. The symbols  $J$ ,  $L$ , and  $S$  stand for the total angular momentum, the orbital angular momentum, and the spin, respectively.

In the geometric unitarization scheme we use, the nuclear-bar phase parameters (in deg) are given by

$$\delta(J, L=J, S=0) = (180/\pi)f_0^J, \quad (\text{A5a})$$

$$\delta(J, L=J, S=1) = (180/\pi)f_1^J, \quad (\text{A5b})$$

$$\delta(J, L=J-1, S=1) = (180/\pi)f_{L=J-1}, \quad (\text{A5c})$$

$$\delta(J, L=J+1, S=1) = (180/\pi)f_{L=J+1}, \quad (\text{A5d})$$

$$\epsilon_J = (180/\pi)f_{J-1, J+1}. \quad (\text{A5e})$$

The one-boson-exchange contributions to the  $f$ 's follow.

#### A. Pseudoscalar ( $J=0^-$ ) Born Term

The  $J=0^-$  Born term is defined by the interaction Lagrangian

$$\mathcal{L}^{\text{int}} = (4\pi)^{1/2} g \bar{\psi} \gamma_5 \psi \phi^{(p)}, \quad (\text{A6})$$

where  $\phi^{(p)}$  is the pseudoscalar field and  $g$  is the meson-nucleon coupling constant. Then

$$f_0^J = g^2(p/4E)[(x_0-1)Q_J(x_0) - \delta_{J,0}], \quad (\text{A7a})$$

$$f_1^J = g^2(p/4E)[(x_0+1)Q_J(x_0) - Q_{J+1}(x_0) - Q_{J-1}(x_0)], \quad (\text{A7b})$$

$$f_{L=J-1} = -g^2(p/4E)(2J+1)[Q_J(x_0) - Q_{J-1}(x_0)], \quad (\text{A7c})$$

$$f_{L=J+1} = -g^2(\not{p}/4E)(2J+1)[Q_{J+1}(x_0) - Q_J(x_0)], \quad (\text{A7d})$$

$$f_{J-1, J+1} = -g^2(\not{p}/4E)[J(J+1)]^{1/2}/(2J+1)[Q_{J+1}(x_0) + Q_{J-1}(x_0) - 2Q_J(x_0)]. \quad (\text{A7e})$$

### B. Scalar ( $J=0^+$ ) Born Term

The  $J=0^+$  Born term is defined by the interaction Lagrangian

$$\mathcal{L}^{\text{int}} = (4\pi)^{1/2} g \bar{\psi} \psi \phi^{(S)}, \quad (\text{A8})$$

where  $\phi^{(S)}$  is the scalar field and  $g$  is the meson-nucleon coupling constant. Then

$$f_0^J = g^2[\not{p}/(8Ea)][(1+a^2-2ax_0)Q_J(x_0) + 2a\delta_{J,0}], \quad (\text{A9a})$$

$$f_1^J = g^2 \frac{\not{p}}{4E} \left[ \frac{1+a^2+2ax_0}{2a} Q_J(x_0) - Q_{J+1}(x_0) - Q_{J-1}(x_0) \right], \quad (\text{A9b})$$

$$f_{L=J-1} = g^2 \frac{\not{p}}{4E(2J+1)} \left\{ \frac{1+a^2+2J(1-a^2)}{2a} Q_{J-1}(x_0) + [2J(ax_0-1)-1]Q_J(x_0) \right\}, \quad (\text{A9c})$$

$$f_{L=J+1} = g^2 \frac{\not{p}}{4E(2J+1)} \left\{ \frac{1-3a^2+2J(1-a^2)}{2a} Q_{J+1}(x_0) + [2J(ax_0-1)+2ax_0-1]Q_J(x_0) - 2a\delta_{J,0} \right\}, \quad (\text{A9d})$$

$$f_{J-1, J+1} = g^2 \frac{\not{p}}{4E} \frac{a[J(J+1)]^{1/2}}{(2J+1)^2} [Q_{J-1}(x_0) - Q_{J+1}(x_0)]. \quad (\text{A9e})$$

### C. Vector ( $J=1^-$ ) Born Term

The  $J=1^-$  Born term is defined by the interaction Lagrangian

$$\mathcal{L}^{\text{int}} = (4\pi)^{1/2} \bar{\psi} [g\gamma_\mu \phi_\mu^{(V)} + (f/4M)\sigma_{\mu\nu}(\partial_\nu \phi_\mu^{(V)} - \partial_\mu \phi_\nu^{(V)})] \psi, \quad (\text{A10})$$

where  $\sigma_{\mu\nu} = \frac{1}{2}i(\gamma_\mu \gamma_\nu - \gamma_\nu \gamma_\mu)$ ,  $\phi^{(V)}$  is the vector field, and  $g$  and  $f$  are the meson-nucleon coupling constants for Dirac and Pauli coupling, respectively. Then

$$f_0^J = -g^2 \left( \frac{\not{p}}{4E} \right) \left\{ \left( 3 + \frac{1+a^2}{2a} \right) Q_J(x_0) - 2 \frac{f}{g} [(x_0-1)Q_J(x_0) - \delta_{J,0}] - \frac{2(f/g)^2}{(1-a)^2} [(x_0-1)(1+a+a^2+ax_0)Q_J(x_0) - (1+a^2+ax_0)\delta_{J,0} - \frac{1}{3}a\delta_{J,1}] \right\}, \quad (\text{A11a})$$

$$f_1^J = -g^2 \left( \frac{\not{p}}{4E} \right) \left\{ 2Q_{J+1}(x_0) + 2Q_{J-1}(x_0) + \frac{1+2a+a^2-4ax_0}{2a} Q_J(x_0) + 2 \frac{f}{g} [Q_{J+1}(x_0) + Q_{J-1}(x_0) - (x_0+1)Q_J(x_0)] + \frac{(f/g)^2}{(1-a)^2} \left\{ 2(3a+x_0+2ax_0+a^2x_0+ax_0^2)Q_J(x_0) - (1+4a+a^2+2ax_0)[Q_{J+1}(x_0) + Q_{J-1}(x_0)] + \frac{4}{3}a\delta_{J,1} \right\} \right\}, \quad (\text{A11b})$$

$$f_{L=J-1} = -g^2 \frac{\not{p}}{4E(2J+1)} \left\{ \frac{1}{2a} [2J(1-a^2) + (1+a)^2]Q_{J-1}(x_0) + 2(3J+1+Jax_0)Q_J(x_0) - 2 \frac{f}{g} \left[ \frac{4J+1+4Ja-a}{1-a} Q_{J-1}(x_0) - \left( 4J+1 + \frac{8Jax_0}{1-a} \right) Q_J(x_0) \right] + \frac{(f/g)^2}{(1-a)^2} [(1+a^2)x_0 + 2J(x_0-1)(1-a^2) + 6a]Q_{J-1}(x_0) + [4Ja^2x_0(x_0-1) + 2(6J-1)a(x_0-1) - 1 - 6a - a^2]Q_J(x_0) - (3 + \frac{1}{3}a^2)\delta_{J,1} \right\}, \quad (\text{A11c})$$

$$f_{L=J+1} = -g^2 \frac{\not{p}}{4E(2J+1)} \left\{ \frac{1}{2a} [2(J+1)(1-a^2) - (1+a)^2]Q_{J+1}(x_0) + 2[3J+2+(J+1)ax_0]Q_J(x_0) - 2a\delta_{J,0} - 2 \frac{f}{g} \left[ \left( \frac{4(J+1)(1+a)}{1-a} - 1 \right) Q_{J+1}(x_0) - \left( 4J+3 + \frac{8(J+1)ax_0}{1-a} \right) Q_J(x_0) + \frac{8a}{1-a} \delta_{J,0} \right] - \frac{(f/g)^2}{(1-a)^2} [x_0(1+a^2) - 2(J+1)(1-a^2)(x_0-1) + 6a]Q_{J+1}(x_0) - [1+6a+a^2+2a(6J+7)(x_0-1) + 4(J+1)a^2x_0(x_0-1)]Q_J(x_0) + [14a+4a^2(x_0-1)]\delta_{J,0} + \frac{8}{3}a^2\delta_{J,1} \right\}, \quad (\text{A11d})$$

$$\begin{aligned}
f_{J-1, J+1} = & g^2 \left( \frac{p}{4E} \right) \frac{[J(J+1)]^{1/2}}{(2J+1)^2} \left[ 2(2J+1)(x_0-1)Q_J(x_0) + (1+a)[Q_{J-1}(x_0) - Q_{J+1}(x_0)] \right. \\
& + 2 \frac{f}{g} \left( 2(2J+1)(x_0-1)Q_J(x_0) + \frac{1+3a}{1-a} [Q_{J-1}(x_0) - Q_{J+1}(x_0)] \right) \\
& + \frac{(f/g)^2}{(1-a)^2} \{ 2(2J+1)(1-a)^2(x_0-1)Q_J(x_0) \\
& \left. + (1+6a-a^2+2a^2x_0)[Q_{J-1}(x_0) - Q_{J+1}(x_0)] - 2a^2\delta_{J,1} \right\}, \quad (\text{A11e})
\end{aligned}$$

The pole projections have been given for isotopic-spin-zero meson exchange. For isotopic-spin-one meson exchange, replace  $\phi$  in the interaction Lagrangian by  $\vec{\tau} \cdot \vec{\phi}$ , and  $g^2$  by  $\vec{\tau}_a \cdot \vec{\tau}_b g^2$ , where  $\vec{\tau}_a$  and  $\vec{\tau}_b$  are  $2 \times 2$  isotopic-spin matrices operating on nucleons  $a$  and  $b$ , respectively. Derivations of these pole projections may be found in a paper by Bryan and Arndt,<sup>15</sup> as well as in other sources cited therein.

#### APPENDIX B: WIDE-MESON EXCHANGE

Consider a wide meson which decays into two pions, as is the case for the  $\rho$  and the  $\epsilon$ . To express the exchange between two nucleons of this wide meson of mass  $m$  and width  $\Gamma$ , we try the following modification of the propagator for the "zero-width" pole term:

$$[m^2 - t]^{-1} \rightarrow [m^2 - t - im\Gamma f(t)]^{-1}, \quad (\text{B1})$$

where  $f(t) = [(t - 4m_\pi^2)/(m^2 - 4m_\pi^2)]^{1/2}$ , and  $t$  is the square of the four-momentum of the exchanged meson. This form of the propagator has a cut in the  $t$  plane from the  $2\pi$  threshold to  $\infty$ , plus poles on the second sheet, resulting in the identities

$$[m^2 - t - im\Gamma f(t)]^{-1} = \int_{4m_\pi^2}^{\infty} dm'^2 P(m'^2) [m'^2 - t]^{-1} \quad (\text{B2})$$

and

$$\int_{4m_\pi^2}^{\infty} dm'^2 P(m'^2) = 1, \quad (\text{B3})$$

where

$$P(m'^2) = \frac{1}{\pi} \frac{m\Gamma f(m'^2)}{(m'^2 - m^2)^2 + m^2\Gamma^2 f^2(m'^2)}. \quad (\text{B4})$$

Note that  $f(t)$  was chosen so that  $P(t)$ , the  $t$  discontinuity of the propagator on the right-hand side of (B1), goes to zero at the two-pion threshold  $t = 4m_\pi^2$ . Comparing Eq. (B2) to

$$[m^2 - t]^{-1} = \int_{4m_\pi^2}^{\infty} dm'^2 \delta(m'^2 - m^2) [m'^2 - t]^{-1}, \quad (\text{B5})$$

we see that the modification of the propagator prescribed by (B1) is equivalent to the replacement of a  $\delta$ -function mass distribution for the exchanged meson by the Breit-Wigner-type mass distribution of Eq. (B4). To an excellent approximation, the peak occurs at  $m'^2 = m^2$ , and the full width at half-maximum is  $\Gamma$ , for the mass distribution weight function  $2m'P(m'^2)$ .

The same choice of propagator, the form given in (B1), when applied to  $\pi\pi$  elastic scattering leads to the  $S$ -matrix element

$$e^{2i\delta_l^{\pi\pi}} = [m^2 - t + im\Gamma f(t)] / [m^2 - t - im\Gamma f(t)] \quad (\text{B6})$$

or

$$\tan \delta_l^{\pi\pi} = \frac{m\Gamma}{m^2 - t} \left( \frac{t - 4m_\pi^2}{m^2 - 4m_\pi^2} \right)^{1/2}, \quad (\text{B7})$$

corresponding to

$$\lim_{t \rightarrow 4m_\pi^2} \delta_l^{\pi\pi} = 0 \quad (\text{B8})$$

and

$$\lim_{t \rightarrow m^2} \delta_l^{\pi\pi} = \frac{1}{2}\pi, \quad (\text{B9})$$

as we should expect for the actual  $\pi\pi$  phase shift. Furthermore, from Eqs. (B2)–(B4),  $\Gamma$  corresponds to the width for decay of the wide meson into  $\pi + \pi$ . Thus the form on the right-hand side of (B1) seems plausible.

We note that for meson-exchange poles well away from the physical region (i.e., not near the negative  $t$  axis, for  $N$ - $N$  elastic scattering), the partial-wave projections of pole terms are not sensitive to the form in which the width is incorporated into the pole term. In fact, there is little sensitivity to the value of the width itself. (In low-energy  $N$ - $N$  elastic scattering, increasing the width is very similar to shifting downward the mass of a zero-width exchanged meson.) We have assumed a width  $\Gamma \lesssim \frac{1}{2}m$ , and that the partial-wave projections are evaluated in the physical region. With these considerations in mind, we use the modification (B1) for the propagator to describe the  $N$ - $N$  scattering amplitude, only for convenience we use a two-pole approximation suggested by Gersten<sup>16</sup>:

$$\begin{aligned}
\left\{ m^2 - t - im\Gamma \left( \frac{t - 4m_\pi^2}{m^2 - 4m_\pi^2} \right)^{1/2} \right\}^{-1} \\
\approx A_1/(m_1^2 - t) + A_2/(m_2^2 - t), \quad (\text{B10})
\end{aligned}$$

where

$$A_1 = \frac{m_1^2 - \Lambda^2}{m_1^2 - m_2^2}, \quad A_2 = \frac{\Lambda^2 - m_2^2}{m_1^2 - m_2^2}, \quad (\text{B11})$$

and  $m_1$ ,  $m_2$ , and  $\Lambda$  are determined by requiring that the approximation (B10) be exact for (1)  $t=0$ , (2) the slope in  $t$  as  $t \rightarrow 0^-$ , and (3)  $t = -m^2$ , all within the physical region for  $N$ - $N$  scattering. We get

$$(1) \Rightarrow m_1^2 m_2^2 = (m^2 + 2m_\pi \Gamma') \Lambda^2, \quad (\text{B12})$$

(B12) and (2)

$$\Rightarrow m_1^2 + m_2^2 = m^2 + 2m_\pi \Gamma' + \Lambda^2 (1 + \Gamma'/4m_\pi), \quad (\text{B13})$$

(B12), (B13), and (3)

$$\Rightarrow \Lambda^2 = m^2 \left[ \frac{(m^2 + 4m_\pi^2)^{1/2} - 2m_\pi}{(m^2/4m_\pi) + 2m_\pi - (m^2 + 4m_\pi^2)^{1/2}} \right], \quad (\text{B14})$$

where  $\Gamma' = m\Gamma/(m^2 - 4m_\pi^2)^{1/2}$ . Equations (B11)–(B14) can easily be solved to yield  $A_1$ ,  $A_2$ ,  $m_1$ , and  $m_2$ .

We thus approximate the exchange of a wide meson with coupling to the nucleon of  $g^2$  by a sum of two zero-width mesons of masses  $m_1$  and  $m_2$  and couplings  $A_1 g^2$  and  $A_2 g^2$ , respectively. For the  $\rho$  exchange, with  $m_\rho = 765 \text{ MeV}/c^2$  and  $\Gamma_\rho = 117 \text{ MeV}$ , we take

$$m_1 = 612 \text{ MeV}/c^2, \quad A_1 g^2 = 0.360 g_{NN\rho}^2 \quad (\text{B15})$$

and

$$m_2 = 994 \text{ MeV}/c^2, \quad A_2 g^2 = 0.640 g_{NN\rho}^2.$$

For the  $\epsilon$  exchange, with  $m_\epsilon = 715 \text{ MeV}/c^2$  and  $\Gamma_\epsilon = 370 \text{ MeV}$ , we take

$$m_1 = 508 \text{ MeV}/c^2, \quad A_1 g^2 = 0.275 g_{NN\epsilon}^2 \quad (\text{B16})$$

and

$$m_2 = 1180 \text{ MeV}/c^2, \quad A_2 g^2 = 0.725 g_{NN\epsilon}^2.$$

The two-pole approximation to the wide-meson propagator given in Eq. (B10), due to Gersten, is surprisingly accurate over the range of  $t$  corresponding to  $N$ - $N$  elastic scattering from 0 to 425 MeV. The maximum discrepancy introduced is 1.4% for  $\epsilon$  exchange and 0.35% for  $\rho$  exchange.

\*Work supported in part by the Air Force Office of Scientific Research, Office of Aerospace Research, U. S. Air Force, under Grant No. 69-1817, and in part by the U. S. Atomic Energy Commission.

<sup>1</sup>M. Taketani, S. Nakamura, and M. Sasaki, *Progr. Theoret. Phys.* (Kyoto) **6**, 581 (1951).

<sup>2</sup>P. Cziffra, M. H. MacGregor, M. J. Moravcsik, and H. P. Stapp, *Phys. Rev.* **114**, 880 (1959).

<sup>3</sup>*Progr. Theoret. Phys.* (Kyoto) Suppl. **39** (1967), part I.

<sup>4</sup>G. Breit and R. D. Haracz, in *High Energy Physics*, edited by E. H. S. Burhop (Academic, New York, 1967), Vol. 1, p. 21.

<sup>5</sup>P. S. Signell, *Phys. Rev. Letters* **5**, 474 (1960).

<sup>6</sup>J. Binstock, *Phys. Rev. D* **3**, 1139 (1971).

<sup>7</sup>V. K. Samaranayake and W. S. Woolcock, *Phys. Rev. Letters* **15**, 936 (1965).

<sup>8</sup>S. C. C. Ting, in *Proceedings of the Fourteenth International Conference on High Energy Physics, Vienna, 1968*, edited by J. Prentki and J. Steinberger (CERN, Geneva, Switzerland, 1968), p. 43.

<sup>9</sup>S. R. Deans and W. G. Holladay, *Phys. Rev.* **165**, 1886 (1968).

<sup>10</sup>A. Barbaro-Galtieri, S. E. Derenzo, L. R. Price, A. Rittenberg, A. H. Rosenfeld, N. Barash-Schmidt, C. Bricman, M. Roos, P. Söding, and C. G. Wohl, *Rev. Mod. Phys.* **42**, 87 (1970).

<sup>11</sup>This second-derivative error matrix is based on the data analysis of Ref. 12, and was obtained from one of the authors, Dr. R. A. Arndt, Virginia Polytechnic Institute, Blacksburg, Virginia.

<sup>12</sup>M. H. MacGregor, R. A. Arndt, and R. M. Wright, *Phys. Rev.* **182**, 1714 (1969).

<sup>13</sup>The impact-parameter radii are not to be taken literally. Their meaning is derived from the fact that potential scattering in the Born approximation yields

$$\tan \delta_l \propto \int j_l^2(p r) V(r) r^2 dr$$

(for uncoupled partial waves). The impact parameter  $r = [l(l+1)]^{1/2} \hbar/p$  marks the semiclassical turning point for  $j_l(p r)$ , the solution to the free-wave radial Schrödinger equation. Of course  $j_l^2(p r)$  is nonzero for radii both within and beyond the impact parameter  $r$ , so  $r$  represents here the point of nearest approach which contributes significantly to the phase shift, given reasonable potentials.

<sup>14</sup>M. Derrick, in *High Energy Physics*, edited by K. T. Mahanthappa, W. D. Walker, and W. E. Brittin (Colorado Univ. Press, Boulder, 1969), p. 291. The value given is  $\Gamma_\epsilon \sim 400 \text{ MeV}$ .

<sup>15</sup>R. A. Bryan and R. A. Arndt, *Phys. Rev.* **150**, 1299 (1966).

<sup>16</sup>A. Gersten (private communication).